Virtual screening of natural compounds as interleukin-6 inhibitors to cure covid-19

A dissertation

submitted in partial fulfilment of the requirement

For the award of degree of

Masters of Technology

In

Biotechnology

(June, 2022)

Under the guidance of

Dr. Atul Kumar Upadhyay

Submitted by

EVA RATHI

Roll No. 602004007

DEPARTMENT OF BIOTECHNOLOGY

THAPAR INSTITUTE OF ENGINEERING AND TECHNOLOGY, PATIALA

ACKNOWLEDGEMENT

I am indebted to Dr. Prakash Gopalan, Director, Thapar institute of Engineering and Technology (TIET) for providing the opportunity and facilities of institute to give me a chance to carry out dissertation work as part of M.Tech curricular requirement. With great reverence, I express my warmest feeling with deep sense of gratitude to Dr. Atul Kumar Upadhyay, Assistant Professor, TIET, who agreed to take upon and guided for this dissertation and training. I have no word to express my heartfelt thanks to him for his illuminating guidance, unfailing encouragement, supervision and keen interest during the course of dissertation.

I would like to express my heartfelt respect to HOD, Dr. M S Reddy, Department of Biotechnology, Thapar Institute of Engineering and Technology, Patiala for his kind suggestions and fore-sightedness. I am also thankful to Tanmayee Basu, Ph.D. scholar (TIET), and Arshwinder Singh for their guidance during the whole dissertation work. At the end, thanks to my family and friends for giving me strength to keep going.

DECLARATION

I hereby declare that the project work entitled (**"Virtual screening of natural compounds as interleukin-6 inhibitors to cure covid-19"**) is an authentic record of my own work carried out at, Thapar Institute of Engineering and Technology as requirements of 12 months dissertation for the award of degree of Masters of Technology in Biotechnology, under the guidance of Dr. Atul Kumar Upadhyay, during July, 2021 to July, 2022.

(Signature of student)

EVA RATHI

602004007

CERTIFICATE

This is to certify that Project Dissertation entitled ("**Virtual screening of natural compounds as interleukin-6 inhibitors to cure covid-19**") which is submitted by Eva Rathi for the award of degree of Masters of Technology in Biotechnology, at, Thapar Institute of Engineering and Technology as requirements of 12 months dissertation, the matter embodied in this dissertation has not been submitted to award of any Degree or certificate in any other university/institute.

Date: July 28, 2022

Dr. Atul Kumar Upadhyay
(Assistant Professor)

TABLE OF CONTENTS

LIST OF FIGURES

LIST OF TABLES

ABSTRACT

A global health problem has been identified with the COVID-19 outbreak of the coronavirus, which is brought on by the SARS-CoV-2 virus. Identification of novel treatments was urgently required. This dissertation examines virtual screening of natural compounds that can act as interleukin-6 inhibitors so as to cure COVID-19. Identification of the potential active site of the target protein Interleukin-6 was done using PrankWeb. For virtual screening, 10 natural compounds were downloaded from PubChem. Structure Data File (SDF) format was used to download these compounds. 10 Compounds that were selected for virtual screening were Telmisartan, Candesartan, Ivermectin, Nafamostat, Salvianolic Acid, Favipiravir, Tipranavir, Olmesartan, Losartan and Arbidol. Virtual screening of 10 compounds was done using AutoDock Vina in PyRx software, for visualization of interacting residues of docked complexes PyMOL was used. To predict the ADME and drug likeness SwissADME was used and for ADMET and the pharmacokinetic properties admetSAR was used. Molecular dynamic simulation was executed to check the stability of the conformation using GROMACS 2020.1 software where we found out the Root Mean Square Deviation, Root Mean Square Fluctuation, Radius of Gyration and SASA graphs for further analysis.

OBJECTIVES

1. Virtual screening of natural compounds to act as Interleukin-6 blockers.

2. Docking studies and drug likeness properties of screened molecules against Interleukin-6.

3. Molecular dynamics studies of the bound complex to check its stability.

CHAPTER -1 INTRODUCTION

COVID-19 came out as a major life threat to the world, started from Wuhan (China) in early December of 2019. (Loeffelholz & Tang, 2020). As of, 16 May 2022 over 51.7 crores and 62.6 lakh deaths have been reported worldwide (WHO, 2022). COVID-19 is an infectious disease caused by SARS-CoV-2 virus (Rodriguez et al., 2020). Spreading rapidly and having high mortality rate has caused major obstructions (Zhu et al., 2020). Respiratory system is primarily affected by SARS-CoV-2 virus, making other organs also a part of the infection. Infection in the lower respiratory tract which included symptoms like fever, dry cough and shortness of breath were analysed at the start of cases from Wuhan, China (Huang et al., 2020).

Coronaviruses single stranded RNA viruses of ~30 kb. A wide variety of host species are infected by it (Channappanavar et al., 2014). They are categorised into four genera; α, β, γ, and δ on the basis of their genomic structures. Mammals are infected by α and β coronaviruses (Rabi et al., 2020). 229E and NL63 are human coronaviruses which belong to α coronaviruses and are responsible for cold and cough. β coronaviruses consists of SARS-CoV, Middle East respiratory syndrome coronavirus (MERS-CoV) and SARS-CoV-2.

Fibroblasts, Keratinocytes, Mesangial cells, Vascular endothelial cells, Mast cells, Macrophages, Dendritic cells, T and B cells, and leukocytes all produce interleukins. Interleukins are involved in immune cell proliferation, activation, differentiation, migration, maturation, and adhesion. It has anti-inflammatory as well as pro-inflammatory characteristics. They are a wide set of proteins that bind to high-affinity receptors on cell surfaces and cause a variety of responses in tissues and cells (Akdis et al., 2011).

Most interleukins are encoded by messenger RNA, which is unstable and causes transitory production. These compounds are promptly secreted when they have been produced. Interleukin responses include up- and down-regulatory processes, as well as the stimulation and involvement of genes that encode cytokine receptor inhibitors (Zhu et al., 2017).

There are various Interleukins which includes **Interleukin-1 (IL-1), Interleukin-2 (IL-2), Interleukin-3 (IL-3), Interleukin-4 (IL-4), Interleukin-5 (IL-5), Interleukin-6 (IL-6), Interleukin-7 (IL-7), Interleukin-8 (IL-8), Interleukin-9 (IL-9), and Interleukin-10 (IL-10).**

Major function of these interleukins is B and T-cell differentiation, proliferation, selection and stimulation (Belghith et al., 2018). Hence, analysing natural compounds to block interleukin-6 is essential to upgrade our knowledge and cure COVID-19.

1.1 Role of INTERLEUKIN- 6

Interleukin-6 (IL-6) is a multifunctional cytokine that was discovered to be a B-cell differentiation factor that causes antibody-producing cells to mature. IL-6 has a variety of other functions, including impacts on blood vessels, T cells, and neurons. IL-6 is also linked to the activity of other cytokines, such as leukemia-inhibitory factor and ciliary neurotrophic factor (Kishimoto, 2006). Many inflammatory disorders, such as systemic lupus erythematosus, systemic juvenile arthritis, Crohn's disease, rheumatoid arthritis (RA), and COVID-19, have elevated IL-6 expression (Gabay, 2006). Patients' symptoms and illness progression can be reduced by inhibiting IL-6.

1.2 IL-6 Mediated Signaling

T cells, B cells, monocytes, fibroblasts, and other cell types produce IL-6, which is a single-chain protein produced by T cells, B cells, monocytes, and other cell types (Nishimoto & Kishimoto, 2006). IL-6, like other IL-6 family members, is organised into four long -helical structures. The IL-6 family includes cytokines such as IL-11, leukaemia inhibitory factor, oncostatin M, ciliary neurotrophic factor, and cardiotrophin-1 (Heinrich et al., 2003).

It has two modes of signalling to cells: trans-signaling with the soluble IL-6 receptor (IL-6R) and traditional receptor-bound signalling. IL-6R and gp130, a signal-transducing transmembrane protein, are required for both types of signaling (Scheller & Rose, 2003).

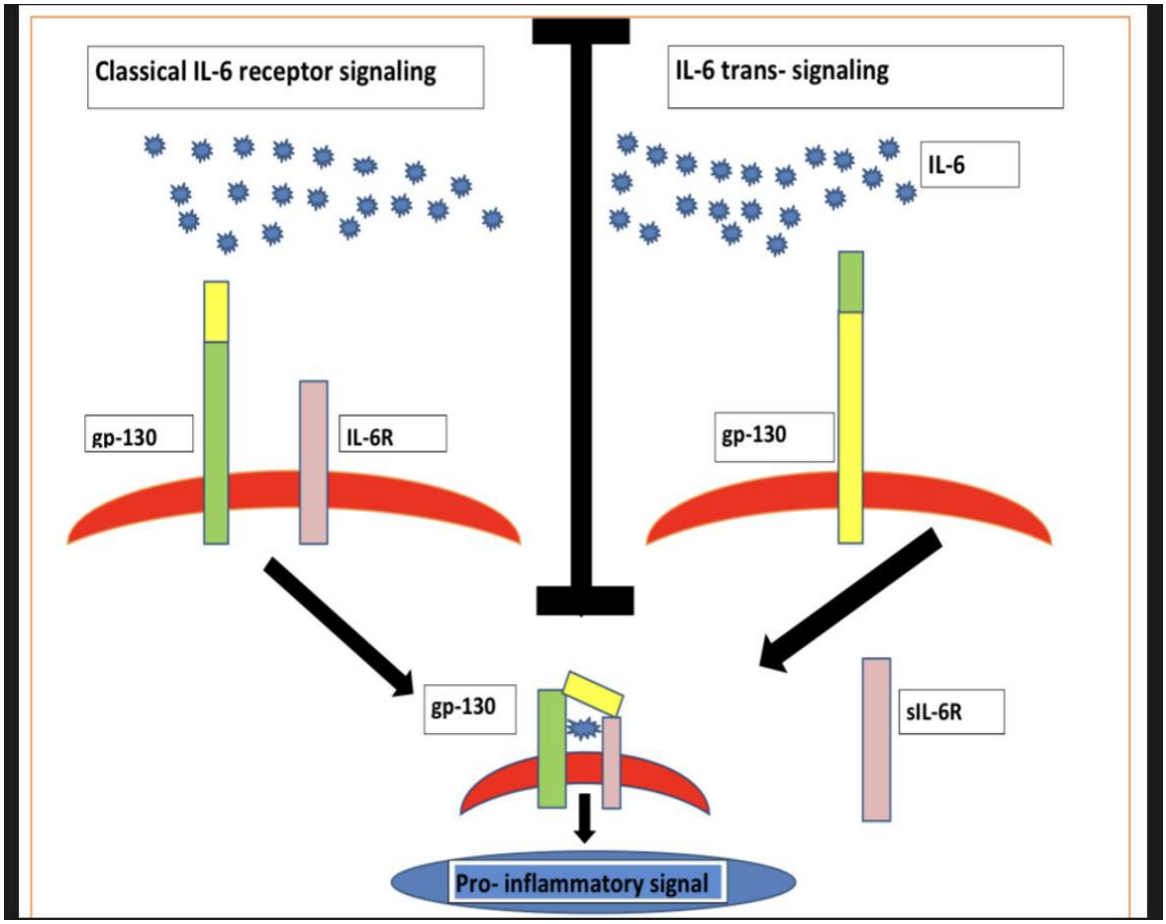

Figure 1: IL-6 mediated signaling pathway

We used in silico analysis and a systematic review to look for natural substances that could help block the Interleukin-6 inhibitor and so reduce the severity of COVID-19. Virtual screening of 15 natural substances was carried out using a molecular docking and molecular dynamics simulation approach in this work. The interactions of the drug and protein moiety were also studied in order to better understand the molecular interactions between medicines and proteins. The findings were judged to be encouraging, indicating that certain medicines may have antiviral action against SARS-CoV-2, which can be further verified in experimental conditions.

CHAPTER-2 REVIEW OF LITERATURE

Coronavirus disease 2019 (COVID-19), which began in Wuhan, China, has spread to practically all countries and areas of the world, becoming one of the most devastating pandemics since the 1918–1920 Spanish flu. An RNA virus is to blame (2019 novel coronavirus or 2019-nCoV or SARS-CoV-2). As of July 13, 2020, there have been a total of 12,768,307 confirmed COVID-19 cases and 566,654 deaths. COVID-19 has a tremendous societal and economic impact worldwide, in addition to its significant morbidity and death and the enormous strain it places on health-care systems (Danwang et al., 2020)

To identify people at risk of serious disease and death, an effective screening method is required. Patients in this situation must be closely monitored and admitted to the hospital as soon as possible. Covid-19 progression is linked to a number of biomarkers, including inflammatory markers like C-reactive protein (CRP), ferritin, fibrinogen, D-dimer, and Interleukin 6 (IL-6) (Ponti et al., 2020). According to available evidence, IL-6 outperforms CRP and other inflammatory indicators in diagnosing respiratory distress in Covid-19 (Herold et al., 2020).

In Covid-19, IL-6 appears to be the primary driver of immunological dysregulation and ARDS (Magro, 2020). The introduction of monoclonal antibodies (mAbs) that block certain cytokine receptors, like Tocilizumab and Sarilumab, into medical practice has been a significant step forward in the treatment of IMIDs (Kang et al., 2019), and more recently, in the care of severely ill patients with CSS, such as COVID-19 (Koch et al., 2019).

So according to the contextual (9 studies, 1426 patients), people with acute COVID-19 had considerably higher IL6 concentrations than patients with mild COVID-19 (mean difference was 38.6 pg/ml; p 0.001). Elevated IL-6 concentrations were related with a substantial increase in mortality ($p = 0.03$), according to meta-regression. When IL-6 concentrations exceed 55 pg/ml, the chance of severe COVID-19 increases, as does the risk of death (Aziz et al., 2020).

By attaching to the transmembrane (cis-signaling) or soluble form (trans-signaling) of the IL-6 receptor (IL-6R) then associating with membrane-bound gp130, IL-6 triggers the downstream Janus kinase (JAK) signal (Johnson et al., 2018). The maturation of naive T cells into effector T cells, the induction of vascular endothelial growth factor (VEGF) expression in epithelial cells, the increase in vessel permeability, and the reduction in myocardium contractility are just a few

biological outcomes of excessive IL-6 signalling that result in organ damage (Tanaka et al., 2016).

The US Food and Drug Administration has licenced IL-6 inhibitors (IL6ri) for the treatment of CRS in patients receiving chimeric antigen receptor T-cell therapy. The use of tocilizumab caused individuals with severe COVID-19 to experience a rapid improvement in their symptoms and radiographic abnormalities, according to the findings of an open-label, uncontrolled case series (n=21) (Xu et al., 2020).

The advantages of IL6ri therapy in COVID-19 patients have been further validated by more recent, larger observational trials (Guaraldi et al., 2020). Evidence-based clinical therapy during this pandemic, however, does not yet have access to the outcomes of randomised clinical studies.

Interleukin-6 levels have been found to be highly elevated in patients with respiratory dysfunction, and they are closely correlated with the severity of COVID-19 infection (Ulhaq & Soraya, 2020).

In individuals with complex COVID-19 compared to those with noncomplicated illness, interleukin-6 levels were found to be more than three times higher on average, which is associated with a higher risk of mortality (Grifoni et al., 2020). As a result, IL-6 blocking medications have been successfully employed to treat patients with hyper-inflammatory conditions, and strategies to inhibit this cytokine have also been quickly developed (Atal & Fatima, 2020).

In light of this, the biological effects of IL-6 production have been linked to both pro- and anti-inflammatory effects, emphasising IL-6's crucial role in the activation and regulation of the immune response (Scheller et al., 2011).

The critical part IL-6 plays in triggering and controlling the immune response. The biological processes that are impacted by IL-6 production include: regulation of macrophage colony-stimulating factor expression to direct the development of monocytes into macrophages (Chomarat et al., 2000). By engaging with membrane-bound gp130 and binding the transmembrane (cis-signaling) or soluble form (trans-signaling) of the IL-6 receptor (IL-6R), L-6 activates its downstream Janus Kinase (JAK) signal (Johnson et al., 2018).

Numerous naturally occurring substances derived from plants, particularly phytochemicals, may offer an initial indication for the use of plant extracts in IL-6 suppression. With their abundance of chemical diversity and anti-inflammatory properties, phytochemicals may be useful as therapeutic agents against COVID-19 infection. Plants may offer various, affordable sources of medications that help standardise IL-6 levels (Mani et al., 2020).

CHAPTER-3 MATERIALS AND METHODS

3.1 Protein structure resources

The related structural information of the Interleukin-6 (IL-6) (PDB ID: 1IL6) were collected from RCSB database (https://www.rcsb.org/).

3.2 Pocket detection and selection

Active site prediction is required to identify the precise functional component of a protein. PrankWeb was used to identify the potential active site of the target protein Interleukin-6 (1IL6).

3.3 Ligand selection and preparation

For virtual screening, antiviral medicines from DrugBank and a dataset of FDA-approved medications from Zinc15 library were downloaded. Structure Data File (SDF) format was used to download these compounds. Different file formats were converted using the Open Babel (http://openbabel.org) programme. All molecules were initially converted to AutoDock Ligand (PDBQT) format and compound energy was minimised using PyRx.

3.4 Virtual screening

The reported crystal structure of Interleukin-6 was used for virtual screening (PDB ID: 1IL6). Virtual screening was carried out with PyRx 0.8 and AutoDock Vina (Trott & Olson 2010). The entire protein surface was docked with the substances that lacked any designated binding sitesThe value of the grid box was set to center x= 40, center y=40 and center z= 40
with an exhaustiveness value of 8 by default.

The docked complexes with the lowest binding affinity values underwent additional investigation using PyMOL to examine interactions between hydrogen and hydrophobic bonds. The potential for using the resultant ligands as medication candidates is very high.

3.5 Molecular features analyses

SwissADME (http://www.swissadme.ch/) was used to predict compounds' ADME and drug-likeness. Compound input for the SwissADME web application has been provided by SMILES (Simplified Molecular Input Line Entry System). To further ensure the druggability potential of

compounds, ADMET and the pharmacokinetic features were assessed utilising the admetSAR web server (http://lmmd.ecust.edu.cn/admetsar2).

3.6 Molecular Docking

Autodock Vina, server was used for molecular docking (https://vina.scripps.edu/downloads/). It is an online server created and maintained by Dr. Oleg Trott in the Molecular Graphics Lab (now CCSB) at The Scripps Research Institute. Finally selected potential natural compounds structure was uploaded as a ligand whereas Interleukin-6 structure procured from protein data bank was uploaded as receptor onto the server.

3.6.1 Steps involved in Molecular Docking

1- Downloading the protein PDB file

2- Downloading ligand file from PubChem in SDF format

Open in pymol and save file in PDB format

Open in autodock MGL tools through ligand file

Ligand then torsion rootand then detect root

Ligand eventually output and can save as PDBQT

3- Opening protein file in MGL tools for Editing- deletion of water- adding polar H- adding charges (kolman charge)

Grid- macromolecule- choose file- save PDBQT file

4- Running receptor (file name).pdbqt

ligand(file name).pdbqt

Config (config file name).txtt

Log log.txt

Out output.pdbqt

5- cd(folder extension link) "(vina folder extension)\ vina.exe

3.7 Molecular Dynamics Simulation

Using the software GROMACS 2020.1, MD simulations of the best docked outcomes with the lowest binding energies were performed. Protein and ligands made up the simulation system's components. CHARMM36 force field was used to run all of the MD simulations (Huang et al., 2016).

3.7.1 Steps involved in MD Simulation

CREATE INITIAL STATE

>Cleaning the molecule to get rid of the ligand atoms and water molecules.

(i) Remove water molecules

grep -v HOH complex.pdb> complex_clean.pdb

(ii) Remove ligand atoms to save in separate .pdb file

grep LIG1 complex_clean.pdb> unk1.pdb

NOTE: Open the complex_clean.pdb file in text format and remove all the co- ordinates of the nonamino- acid entities.

3. GENERATE TOPOLOGY FOR PROTEIN WITH pdb2gmx

(i) Download the latest CHARMM36 force field from the MacKerell lab website (http://mackerell.umaryland.edu/charmm_ff.html#gromacs).

>There should be a "charmm36-mar2019.ff" subdirectory in the working directory.

(ii) Prepare the topology with pdb2gmx

gmx pdb2gmx -f complex_clean.pdb -o complex_processed.gro

NOTE1: Select the desired force field when prompted to choose a force field.

NOTE2: Choose the default water model when prompted.

4. GENERATE TOPOLOGY FOR LIGAND USING EXTERNAL TOOLS

(i) Add hydrogen atoms to LIG1

> To produce a .mol2 file and add H atoms, use the OpenBabel program.

(ii) Open lig1.mol2 file in a plain text editor and change the MOLECULE heading.

>Replace "*****" with "LIG1".

(iii) Sort the bond order in the @<TRIPOS>BOND section.

>download the sort_mol2_bonds.pl script

(http://www.mdtutorials.com/gmx/complex/Files/sort_mol2_bonds.pl) and execute it:

perl sort_mol2_bonds.pl lig1.mol2 lig1_fix.mol2

(iv) Prepare the LIG1 Topology with CGenFF

> upload the lig1_fix.mol2 file in the cgenff server (https://cgenff.umaryland.edu/)

> save the contentents from topology in the form of a CHARMM "stream" file as lig1.str

(v) Create topology

python cgenff_charmm2gmx_py2_nx1.py LIG1 lig1_fix.mol2 lig1.str charmm36-mar2019.ff

NOTE: download the "cgenff_charmm2gmx.py" conversion script from the MacKerell lab website (http://mackerell.umaryland.edu/charmm_ff.shtml#gromacs) before performing the conversion.

5. BUILD A COMPLEX

(i) Convert the "lig1_ini.pdb" from cgenff_charmm2gmx.py file to .gro format with editconf:

gmx editconf -f lig1_ini.pdb -o lig1.gro

(ii) Copy the contents of the complex_processed.gro file and paste it into a new file, name it as "complex.gro".

> Copy the coordinate section of unk1.gro and paste it into complex.gro, below the last line of the protein atoms, and before the box vectors.
> Since we have added more atoms into the .gro file, increase the second line of complex.gro to reflect the change in total number of atoms.

(iii) Build the topology

> Include the LIG1 ligand parameters in the system topology "topol.top" file. Insert the line that says #include "lig1.itp" into topol.top after the position restraint file is included.
> Adjust the [molecules] directive and add the UNK1 molecule in the complex.gro.

6. ADD BOX AND SOLVATION TO THE SYSYTEM

(i) Define the unit cell around the complex

```
gmx editconf -f complex.gro -o newbox.gro -bt dodecahedron -d 1.0
```

(ii) Solvate the cell and fill it with water

```
gmx solvate -cp newbox.gro -cs spc216.gro -p topol.top -o solv.gro
```

7. INTRODUCTION TO INTERACTION POTENTIALS

-> Add ions to the sysytem

(i) Copy the parametrs from the link-
"http://www.mdtutorials.com/gmx/complex/Files/ions.mdp" and paste it into a .mdp file

```
nano ions.mdp
```

(ii) Assemble a .tpr file using grompp

```
gmx grompp -f ions.mdp -c solv.gro -p topol.top -o ions.tpr
```

(iii) Pass the .tpr file through genion

```
gmx genion -s ions.tpr -o solv_ions.gro -p topol.top -pname NA -nname CL -neutral
```

NOTE: select the group "SOL" to add ions into.

8. ENERGY MINIMISATION (EM)

(i) Copy the parametrs from the link-
"http://www.mdtutorials.com/gmx/complex/Files/em.mdp" and paste it into a .mdp file

nano em.mdp

(ii) Energy minimisation

gmx grompp -f em.mdp -c solv_ions.gro -p topol.top -o em.tpr

(iii) Running mdrun to carry out EM

gmx mdrun -v -deffnm em -nt 16

(iv) Generating the EM graph

gmx energy -f em.edr -o potential.xvg

(v) Visualising the EM graph

xmgrace potential.xvg

9. EQUILIBRATION OF THE SYSTEM

(i) Implementing restraints in the ligand file

> Generate a position ligand restraint topology

gmx make_ndx -f lig1.gro -o index_lig1.ndx

...

> 0 & ! a H*

> q

> Generate the position restraint

gmx genrestr -f lig1.gro -n index_lig1.ndx -o posre_lig1.itp -fc 1000 1000 1000

NOTE: select the freshly created index group which is group 3 in the index_lig1.ndx file

> Include the position restraint information of the ligand in the topology "topol.top" file. Insert the lines #ifdef POSRES #include "posre_lig1.itp" #endif into the topol.top file after the ligand topology file is included.

> Generate the protein receptor position restraint

gmx make_ndx -f em.gro -o index.ndx

...

> 1 | 13

> q

NOTE: merge the "Protein" and "LIG1" groups.

(ii) Running NVT equilibration

> Copy the parametrs from the link- "http://www.mdtutorials.com/gmx/complex/Files/nvt.mdp" and paste it into a .mdp file

nano nvt.mdp

> Assemble a .tpr file using grompp

gmx grompp -f nvt.mdp -c em.gro -r em.gro -p topol.top -n index.ndx -o nvt.tpr

> Running mdrun for NVT equilibration

gmx mdrun -deffnm nvt -nt 16

(iii) Running NPT equilibration

> Copy the parametrs from the link- "http://www.mdtutorials.com/gmx/complex/Files/npt.mdp" and paste it into a .mdp file

nano npt.mdp

> Assemble a .tpr file using grompp

gmx grompp -f npt.mdp -c nvt.gro -t nvt.cpt -r nvt.gro -p topol.top -n index.ndx -o npt.tpr

> Running mdrun for NPT equilibration

gmx mdrun -deffnm npt -nt 16

11. MD PRODUCTION RUN

>Copy the parametrs from the link- "http://www.mdtutorials.com/gmx/complex/Files/md.mdp" and paste it into a .mdp file

nano md.mdp

> Assemble a .tpr file using grompp

gmx grompp -f md.mdp -c npt.gro -t npt.cpt -p topol.top -n index.ndx -o md_0_22.tpr

> Running mdrun

gmx mdrun -deffnm md_0_22

12. ANALYSIS

(i) Recenter the protein and rewrap the molecules within the unit cell

gmx trjconv -s md_0_22.tpr -f md_0_22.xtc -o md_0_22_center.xtc -center -pbc mol -ur compact

NOTE: Choose "1 (Protein)" for centering and "0 (System)" for output

(ii) Generation of the RMSD graph

gmx rms -s em.tpr -f md_0_22_center.xtc -n index.ndx -tu ns -o rmsd_lig1.xvg

> Visualising the graph

xmgrace rmsd_lig1.xvg

(iii) Generation of RMSF graph

gmx rmsf -s md_0_22.tpr -f md_0_22_center.xtc -o rmsf.xvg

(iv) Generation of the SASA graph

gmx sasa -s md_0_22.tpr -f md_22_center.xtc -o sasa.xvg

(v) Generation of the Radius of Gyration Graph

gmx gyrate -s md_0_22.tpr -f md_0_22_center.xtc -o gyrate.xvg

4.1 Identification of protein structure

Target preparation: From the RCSB Protein Data Bank, the target protein SARS-CoV-2 Interleukin-6, 1IL6.pdb (Jin et al., 2020), was obtained (Burley et al., 2017). The protein was given hydrogens for pH 7.0 and gasteiger charges, and a pdbqt format file was produced using Open Babel (obabel; O'Boyle et al., 2011). Receptor structure in pdbqt format is required by Autodock Vina. Visualization was done using Pymol (Sayle & Milner-White, 1995). By looking at how close they were to the ligand, active site residues were found.

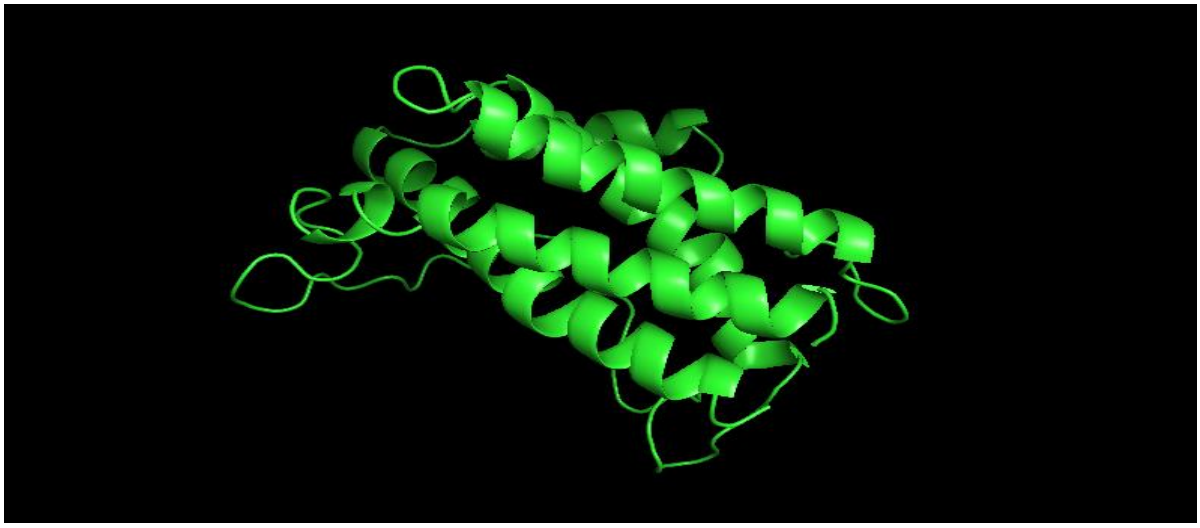

Fig 2: Target Protein Interleukin-6 in pymol

4.2 Pocket detection and selection

Using PrankWeb, it was possible to identify the target protein's putative active site. PrankWeb provides a web interface that enables users to make predictions and visually examine the predicted binding sites using a built-in representation of the sequence-structure. In order to make predictions and display the results, PrankWeb can also determine the input molecule's sequence conservation.

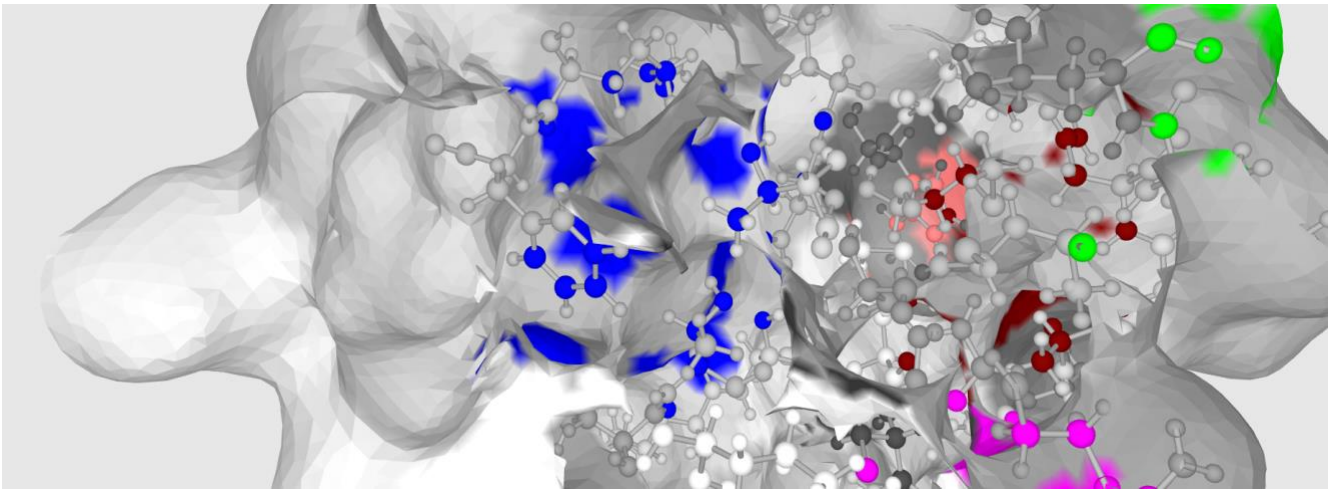

Fig 3: This figure shows a predicted ligand binding site on the surface of Interleukin-6 (1IL6).

4.3 Identification of ligands and its analysis

DrugBank and PubChem were used to get the list and structures of natural compounds. The database version that has 10 natural chemicals in it was downloaded. The 3-dimensional crystal structures collected from PubChem for each molecule. There was structural optimization. The structures were then translated to pdbqt format in order to be used in Autodock Vina's docking computations. The visualisation of the ligands was done using Pymol.

COMPOUNDS
1- Telmisartan
2- Candesartan
3- Ivermectin
4- Salvianolic Acid
5- Favipiravir
6- Nafamostat
7- Olmesartan
8- Tipranavir
9- Losartan
10- Arbidol

Table 1: List of compounds as Interleukin-6 inhibitors

4.4 Docking

Virtual screening workflow was implemented using obabel, Autodock Vina (Trott & Olson, 2010) and customized Python and shell scripts. Pymol and Rasmol were utilized for visualization of the docked results. Autodock Vina was used for docking calculations that did not involve flexible active sites residues.

Docking generated various docked models but the model with lowest binding energy was selected for further analysis. Table below depicts the binding energy of the docked structure and the figures (4-13) shows the docked models.

4.4.1 Telmisartan

Table 2: Docking analysis of Telmisartan

Number of Models	Binding Energy (kcal/mol)
1	-8.0
2	-7.7
3	-7.6
4	-7.4
5	-6.8

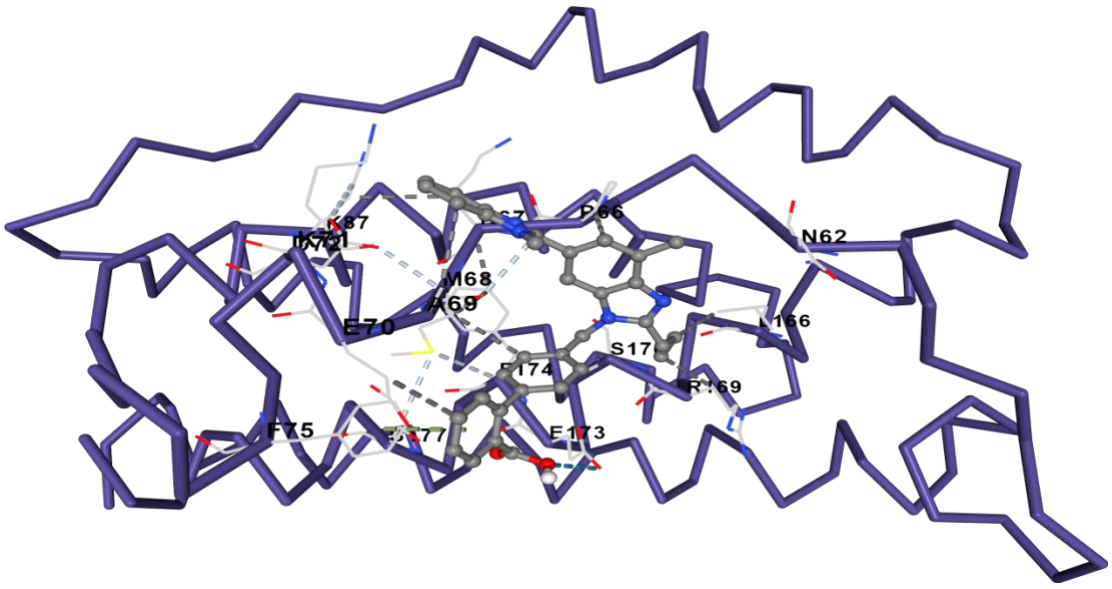

Figure 4: Best Docked structure with highlighted residues of Telmisartan model 1.

4.4.2 Candesartan

Table 3: Docking analysis of Candesartan

Number of Models	Binding Energy (kcal/mol)
1	-7.2
2	-7.0
3	-6.9
4	-6.7
5	-6.6

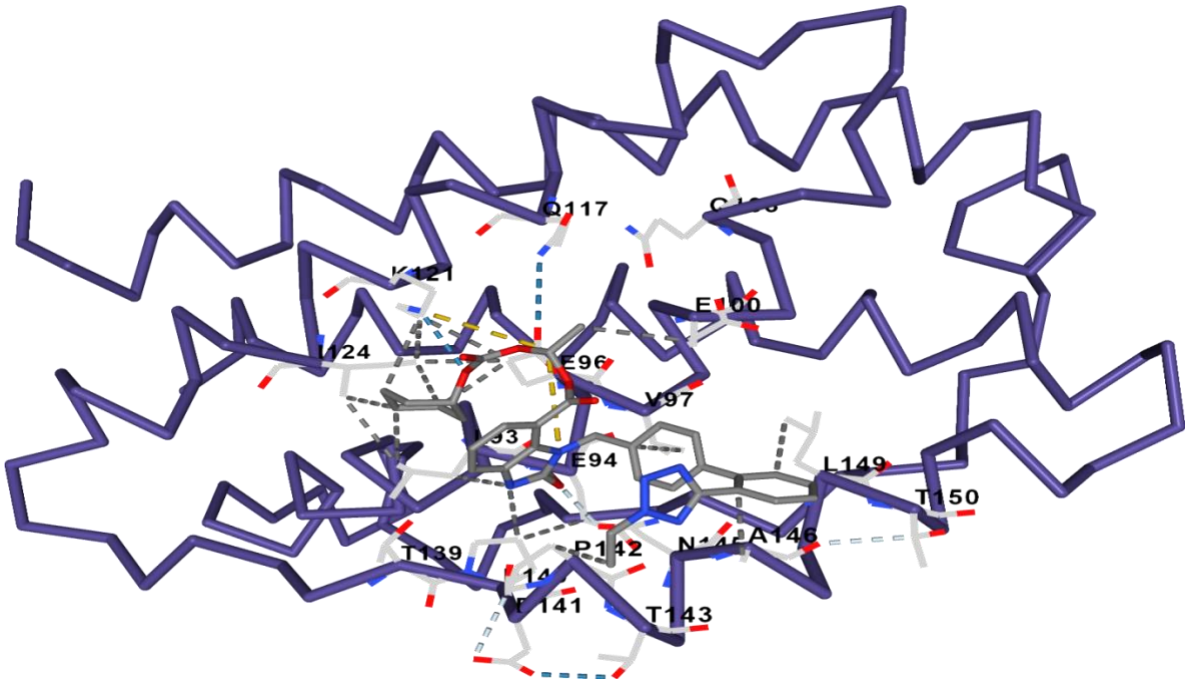

Figure 5: Best Docked structure with highlighted residues of Candesartan model 1.

4.4.3 Ivermectin

Table 4: Docking analysis of Ivermectin

Number of Models	Binding Energy (kcal/mol)
1	-7.5
2	-7.4
3	-6.8
4	-6.7
5	-6.1

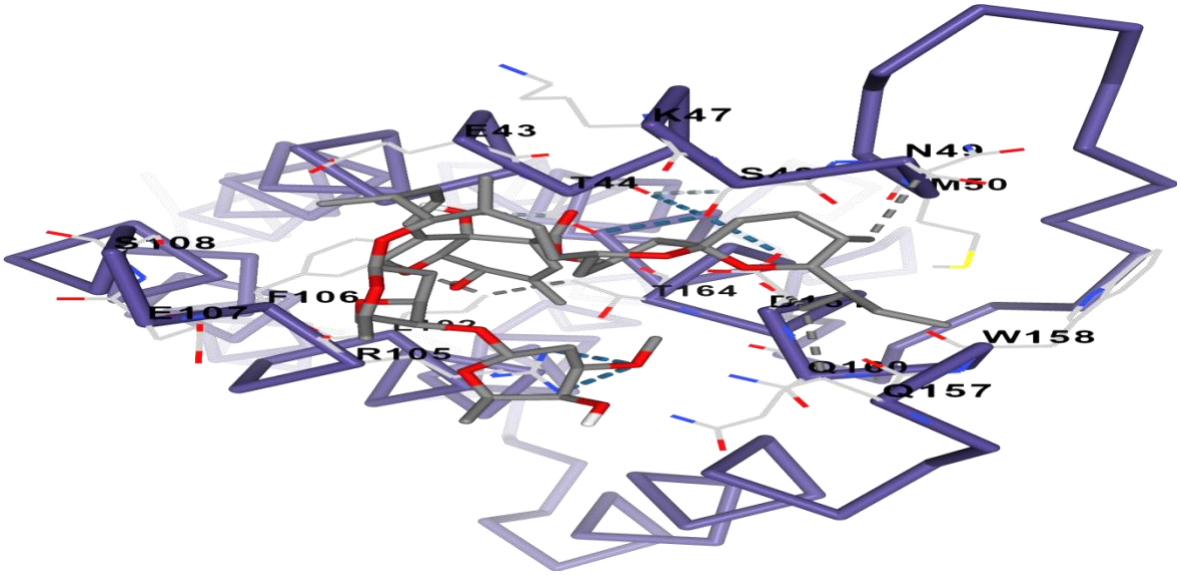

Figure 6: Best Docked structure with highlighted residues of Ivermectin model 1.

4.4.4 Favipiravir

Table 5: Docking analysis of Favipiravir

Number of Models	Binding Energy (kcal/mol)
1	-6.3
2	-6.2
3	-6.1
4	-6.1
5	-5.9

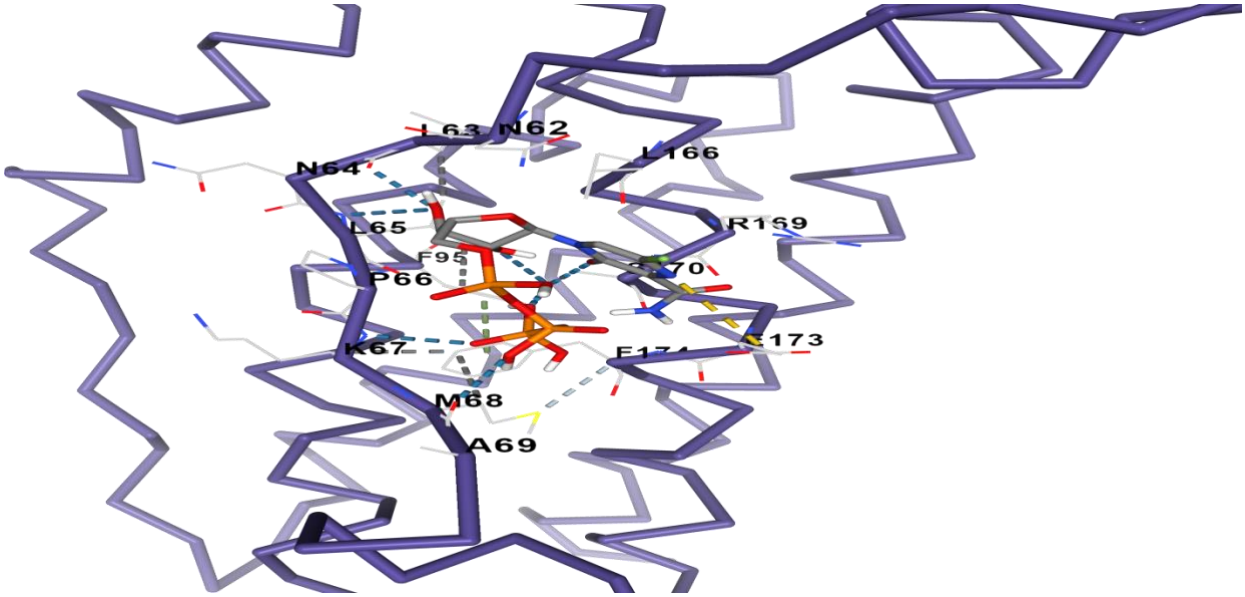

Figure 7: Best Docked structure with highlighted residues of Favipiravir model 1.

4.4.5 Salvianolic Acid

Table 6: Docking analysis of Salvianolic Acid

Number of Models	Binding Energy (kcal/mol)
1	-6.8
2	-6.8
3	-6.6
4	-5.9
5	-5.5

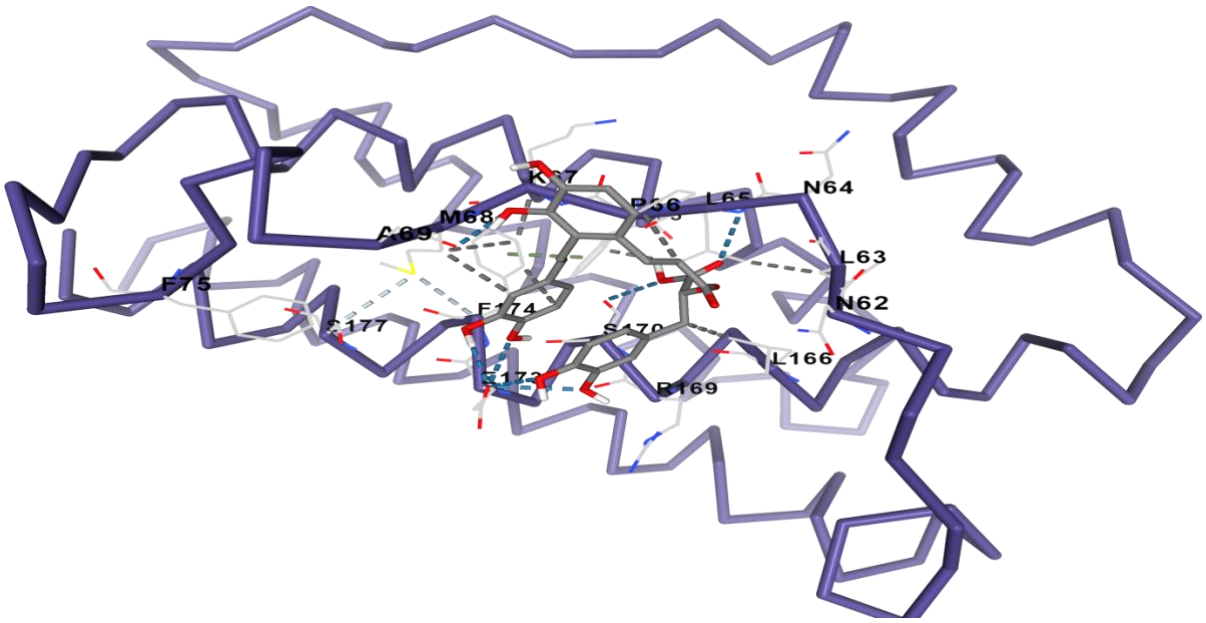

Figure 8: Best Docked structure with highlighted residues of Salvianolic Acid model 1.

4.4.6 Nafamostat

Table 7: Docking analysis of Nafamostat

Number of Models	Binding Energy (kcal/mol)
1	-7.4
2	-7.4
3	-7.2
4	-7.0
5	-6.6

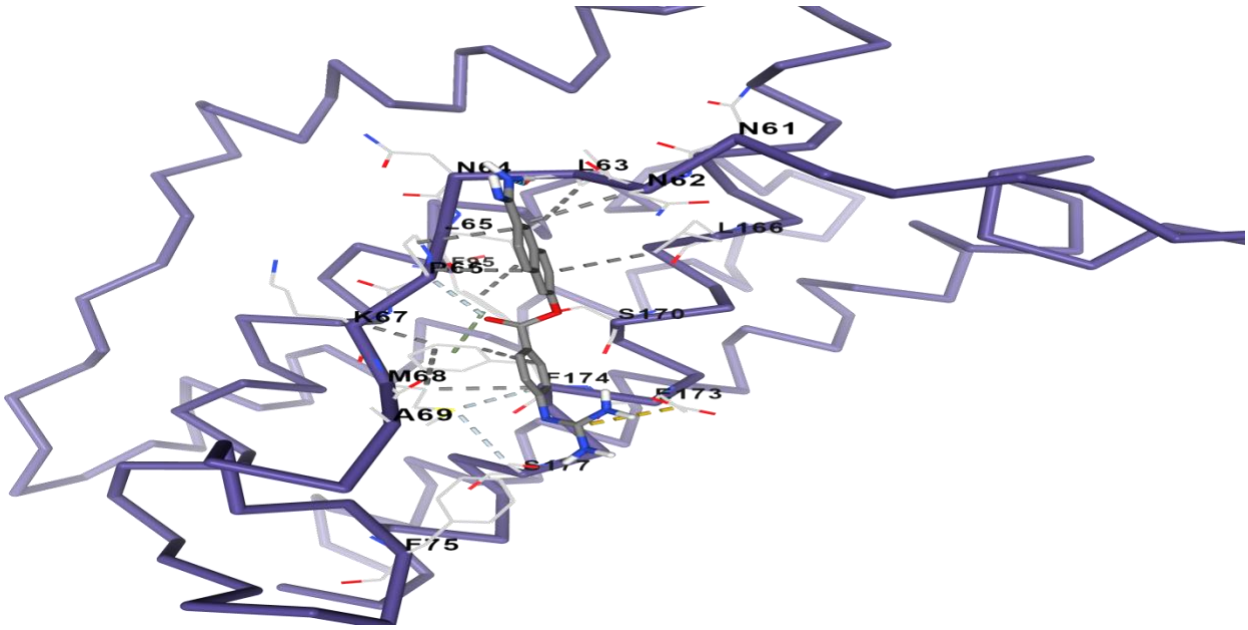

Figure 9: Best Docked structure with highlighted residues of Nafamostat model 1.

4.4.7 Tipranavir

Table 8: Docking analysis of Tipranavir

Number of Models	Binding Energy (kcal/mol)
1	-6.9
2	-6.8
3	-6.7
4	-6.2
5	-5.1

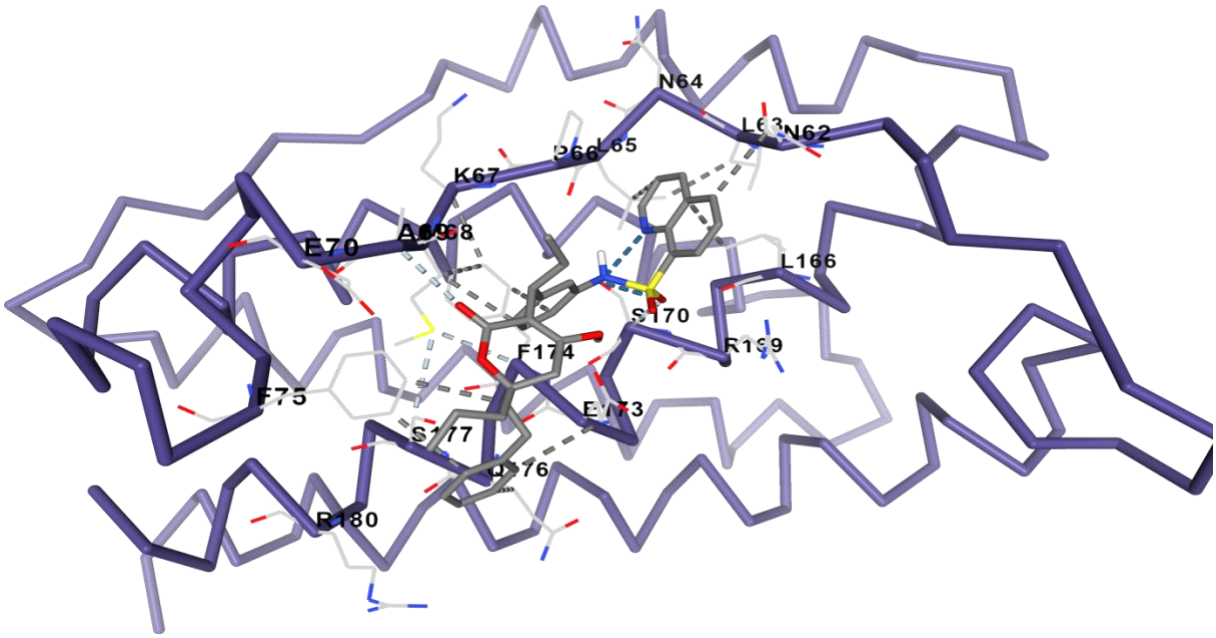

Figure 10: Best Docked structure with highlighted residues of Tipranavir model 1.

4.4.8 Olmesartan

Table 9: Docking analysis of Olmesartan

Number of Models	Binding Energy (kcal/mol)
1	-7.8
2	-7.1
3	-7.1
4	-6.8
5	-6.4

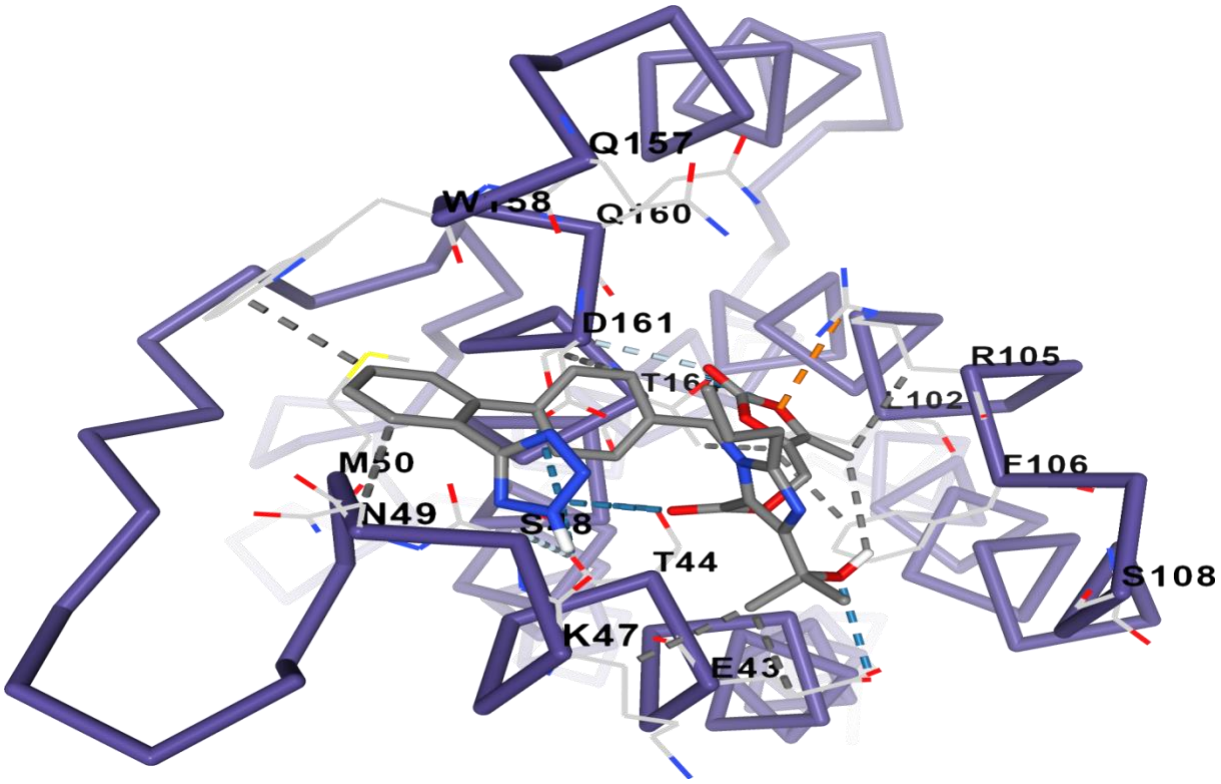

Figure 11: Best Docked structure with highlighted residues of Olmesartan

4.4.9 Losartan

Table 10: Docking analysis of Losartan

Number of Models	Binding Energy (kcal/mol)
1	-7.0
2	-6.6
3	-6.4
4	-6.3
5	-5.6

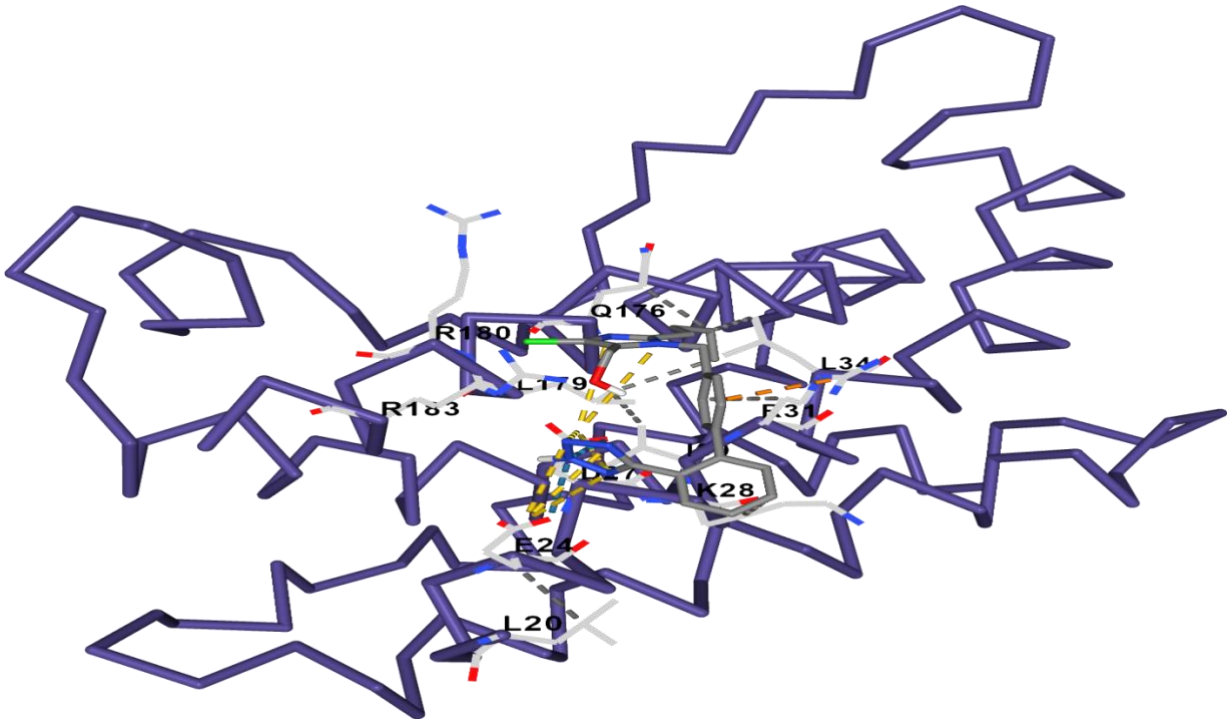

Figure 12: Best Docked structure with highlighted residues of Losartan

4.4.10 Arbidol

Table 11: Docking analysis of Arbidol

Number of Models	Binding Energy (kcal/mol)
1	-5.8
2	-5.6
3	-5.6
4	-5.5
5	-5.2

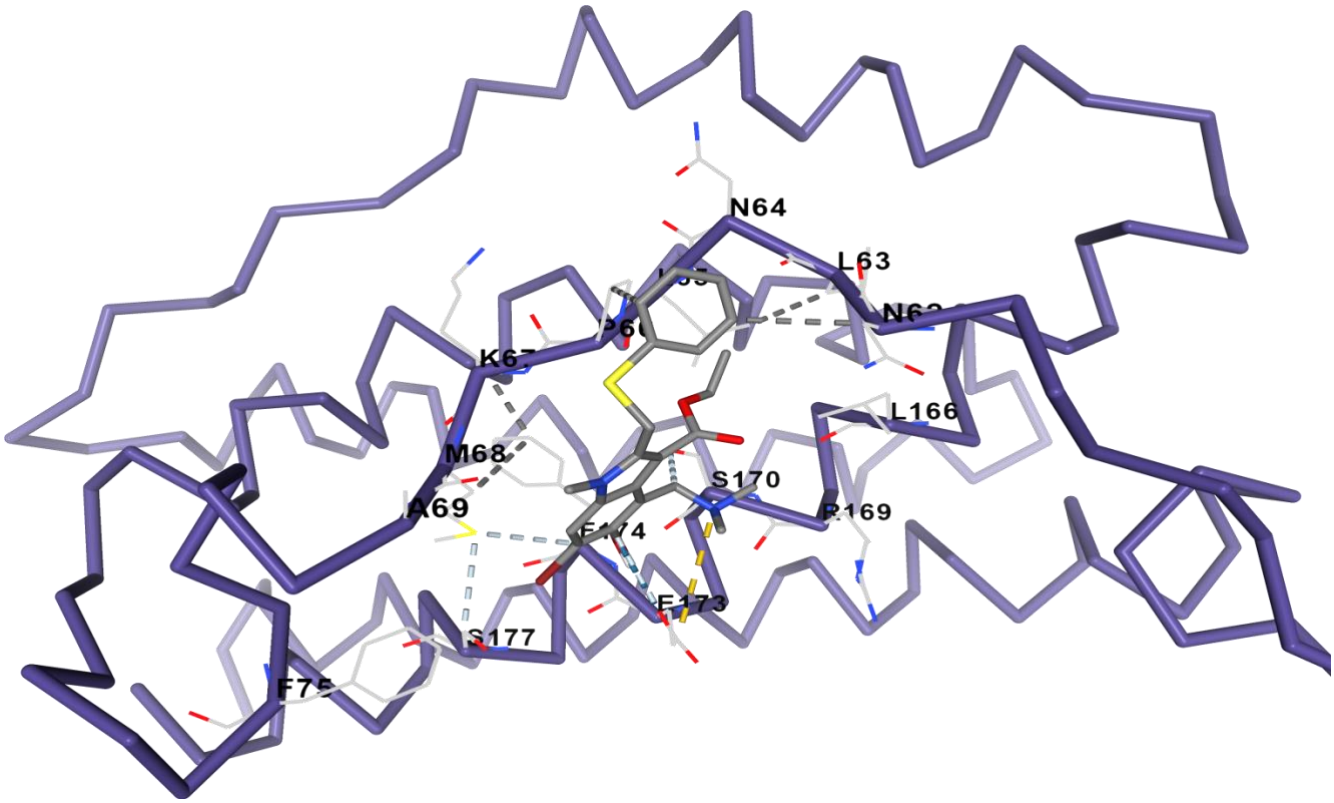

Figure 13: Best Docked structure with highlighted residues of Arbidol

Table 12: Lowest binding energy of all the docking models

Number of Models	Binding Energy (kcal/mol)
Telmisartan	-8.0
Candesartan	-7.2
Ivermectin	-7.5
Favipiravir	-6.3
Salvianolic Acid	-6.8
Nafamostat	-7.4
Tipranavir	-6.9
Olmesartan	-7.8
Losartan	-7.0
Arbidol	-5.8

4.5 Drug Likeness Predictions

The drug-likeness predictions of 10 compounds were carried out using SwissADME. Lipinski 's rule of 5 states that a molecule should meet the following conditions for any ligand to be considered drug-like: molecular weight < 500 Dalton, number of donors of H-bonds < 5, number of acceptors of H-bonds < 10 and LogP < 5 (Lipinski 2004). Out of 10 compounds 6 (Candesartan, Favipiravir, Nafamostat, Olmesartan, Losartan and Arbidol) followed the Lipinski's rule of five and are provided in Table Table 12.

Table 13: Drug-likeness prediction of selected inhibitors of IL-6

Compound	Molecular Formula	Molecular Weight	H−bond acceptors	H−bond donors	TPSA (Topological surface area)	iLOGP	Lipinski violations
Telmisartan	C33H30N4O2	514.62	4	1	72.94	3.88	2
Candesartan	C24H20N6O3	440.45	7	2	118.81	2.44	0
Ivermectin	C48H74O14	875.09	14	3	170.06	5.93	2
Favipiravir	C5H4FN3O2	157.10	4	2	88.84	0.39	0
Salvianolic Acid	C26H22O10	494.45	10	7	184.98	1.62	1
Nafamostat	C19H17N5O2	347.37	4	4	140.57	1.50	0
Tipranavir	C31H33F3N2O5S	602.66	9	2	113.97	3.68	1
Olmesartan	C24H26N6O3	446.50	7	3	129.81	2.04	0
Losartan	C22H23ClN6O	422.91	5	2	92.51	2.59	0
Arbidol	C22H25BrN2O3S	477.41	4	1	80.00	3.79	0

4.6. ADMET Properties

Additionally, admetSAR was used to assess the ADMET characteristics of each of these 10 ligands. All substances demonstrated Blood-Brain Barrier penetration, with the exception of three substances: Ivermectin, Salvianolic Acid, and Losartan. All demonstrated hepatotoxicity. All drugs, with the exception of Telmisartan, were estimated to have class III acute oral toxicity. Except for Arbidol, none of the compounds showed any Caco-2 permeability. Similar intestinal (human) absorption was seen with all substances. Ivermectin contained toxicity evidence for honey bees. Except for Telmisartan, Favipiravir, and Nafamostat compounds, which were non substrates, the majority of the ligands were CYP3A4 substrates. Most docked chemicals have water solubilities greater than -3.

Table 14: ADMET Properties of potential drug candidates

	Te	**Ca**	**Iv**	**Fa**	**Sa**	**Na**	**Ti**	**Ol**	**Lo**	**Ar**
Ames mutagenesis	+	+	-	-	-	-	-	-	-	+
Acute oral toxicity (c)	II	III	III	III	III	III	III	III	III	III
Blood Brain Barrier	+	+	-	+	-	+	+	+	-	+
Caco-2	-	-	-	-	-	-	-	-	-	+
CYP3A4 inhibition	-	+	-	-	-	-	-	+	+	-
CYP3A4 substrate	-	+	+	-	+	-	+	+	+	+
Fish aquatic toxicity	+	+	+	-	+	+	-	+	+	+
Honey bee toxicity	-	-	+	-	-	-	-	-	-	-

Hepatotoxicity	+	+	+	+	+	+	+	+	+	+
Human Intestinal Absorption	+	+	+	+	+	+	+	+	+	+
P-glycoprotein inhibitor	+	+	+	-	+	-	+	+	+	+
P-glycoprotein substrate	+	+	+	-	-	-	+	+	+	-
Subcellular localization	Mito	Mito	Mito	Mito	Mito	Mito	Lyso	Mito	Mito	Lyso
Tetrahymena pyriformis	**1.603**	**1.22**	**0.699**	**0.146**	**0.688**	**1.428**	**1.352**	**0.715**	**1.703**	**1.641**
Water solubility	**-4.094**	**-3.654**	**-4.237**	**-1.651**	**-3.205**	**-3.558**	**-3.836**	**-3.651**	**-3.349**	**-4.368**

+ represents the presence, - represents the absence, Mito represents the mitochondria, Lyso represents the lysosome, Te represents Telmisartan, Ca represents Candesartan, Iv represents Ivermectin, Fa represents Favipiravir, Sa represents Salvianolic Acid, Na represents Nafamostat, Ti represents Tipranavir, Ol represents Olmesartan, Lo represents Losartan, and Ar represents Arbidol.

4.7 Molecular Docking Interactions

Based on the highest binding affinity 5 compounds were chosen for further analysis of interactions of residues.

Table 15: Highest Binding Affinity of Docked Complexes

Compounds	Binding Energy (kcal/mol)
Telmisartan	-8.0
Candesartan	-7.2
Ivermectin	-7.5
Nafamostat	-7.4
Olmesartan	-7.8

4.7.1 Telmisartan had hydrophobic interactions with ALA69, GLU70, LYS71, ASP72, PHE75, LYS87, LEU166, ARG169, SER170, GLU173, and SER177 residues.

4.7.2 Candesartan had hydrophobic interactions with GLN103, GLN117, LYS121, ILE124, THR139, PRO140, ASP141, PRO142, THR143, ASN145, ALA146, LEU149, and THR150 residues.

4.7.3 Ivermectin had hydrophobic interactions with MET50, LEU102, ARG105, PHE106, GLU107, SER108, GLN157, TRP158, GLN160, ASP161, and THR164 residues.

4.7.4 Nafamostat had hydrophobic interactions with PRO66, LYS67, MET68, ALA69, PHE75, LEU166, SER170, GLU173, PHE174, SER177, and LEU65 residues.

4.7.5 Olmesartan had hydrophobic interactions with MET50, ARG105, PHE106, GLN157, TRP158, GLN160, ASP161, and THR164 residues.

4.8 Molecular dynamic simulation studies (MDS)

Telmisartan and Olmesartan were the best dock complexes and subjected to MDS. The conformational stability of the antigen-antibody complex during MD simulation was analyzed by root mean square deviation (RMSD), root mean square fluctuation (RMSF), radius of gyration and Solvent Accessible Surface Area (SASA) plot.

4.8.1 RMSD

The average distance between a group of atoms is indicated by the molecular dynamics metric known as Root Mean Square Deviation (RMSD), which allows the structural distance of a protein to be depicted throughout the course of time. RMSD study of the protein 1IL6 for 22 ns, respectively, with time (ns) on the x-axis and RMSD (nm) on the y-axis.

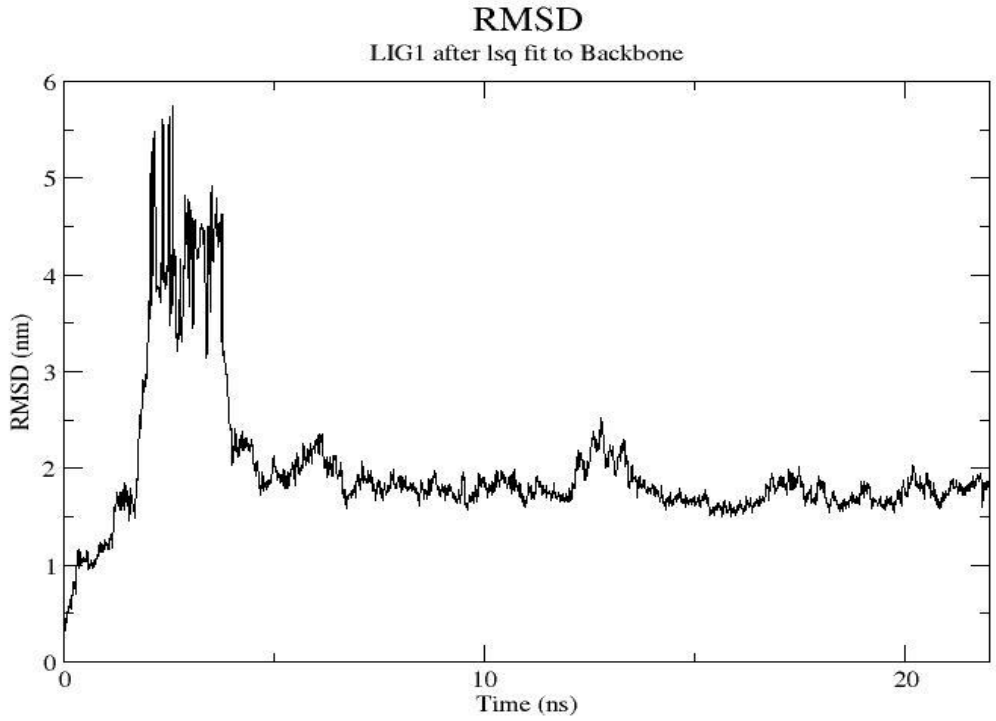

Fig 14: RMSD plot of Telmisartan for the time period of 22 ns: in complex with 1IL6.

The graph analyses the RMSD of Telmisartan for 22ns.

The initial fluctuation was observed between 0 and 1nm and reached upto 6nm and it was the highest fluctuation that was observed throughout the simulation at the beginning. But after 5ns the fluctuations were observed to be stable and remain stable till the end of time except around a spike in fluctuation observed at 13-14ns.

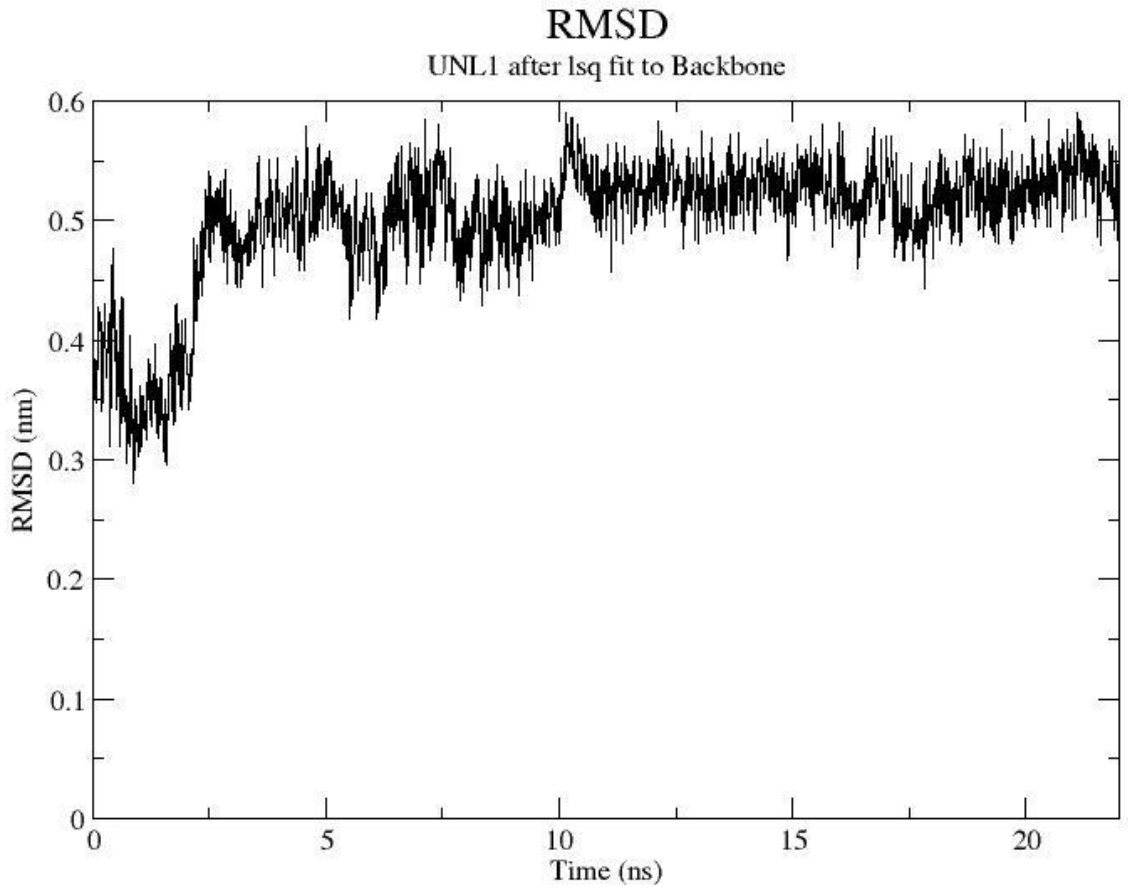

Fig 15: RMSD plot of Olmesartan for the time period of 22 ns: in complex with 1IL6.

The graph analyses the RMSD of Olmesartan for 22ns.

The initial fluctuation was observed between 0.3nm and 0.4nm then spike above 0.4nm and again came down.

A spike in fluctuation was observed above 0.5nm at 5ns. After 5ns the fluctuations dropped a bit and came around 0.4nm. The stability of fluctuations were observed at 10ns till the end of time i.e. 22ns throughout the simulation.

4.8.2 RMSF

The flexibility of individual residues in the protein is often assessed using the Root Mean square Fluctuation (RMSF) metric. We can describe the fluctuations or motions of a certain residue throughout a simulation. For residue number vs. Rmsf, RMSD is unusually plotted (nm). Plotting the graph made it simple to identify which amino acid residue in a protein is in charge of the motion.

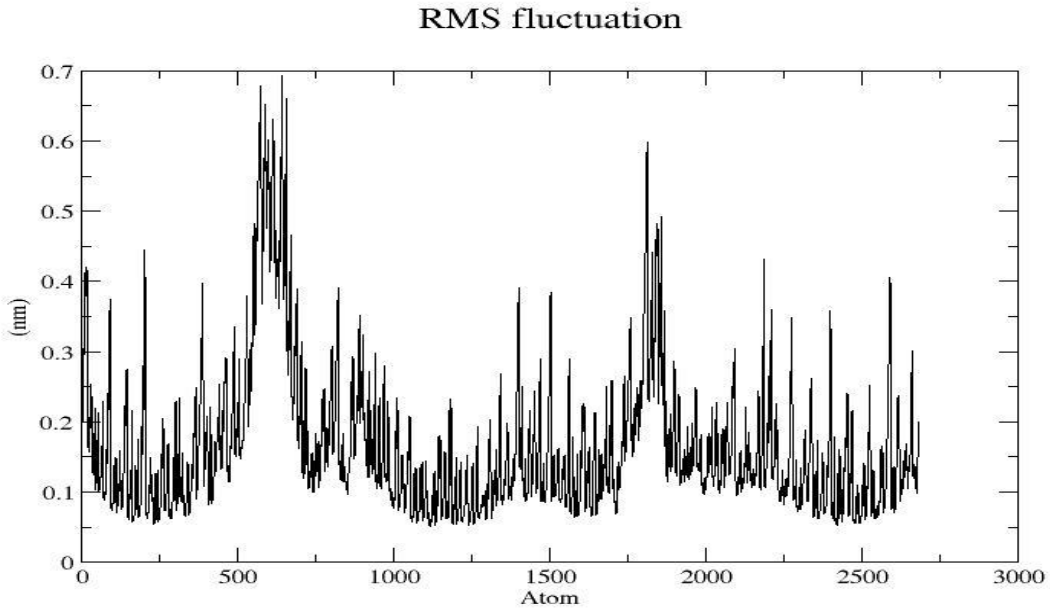

Fig 16: RMSF analysis in Telmisartan

The graph analyses the RMSF fluctuation of Telmisartan for 22ns.

The RMSF showed the graph for RMSF (nm) vs Atom

The initial fluctuation was observed at 0.4nm and then dropped to 0.2nm and kept fluctuating during the whole simulation. The highest fluctuation was observed at around 0.7nm on atoms between 5 00-530 and dropped on atome no.550. The second highest fluctuation was observed between atom no. 1500 and 2000.

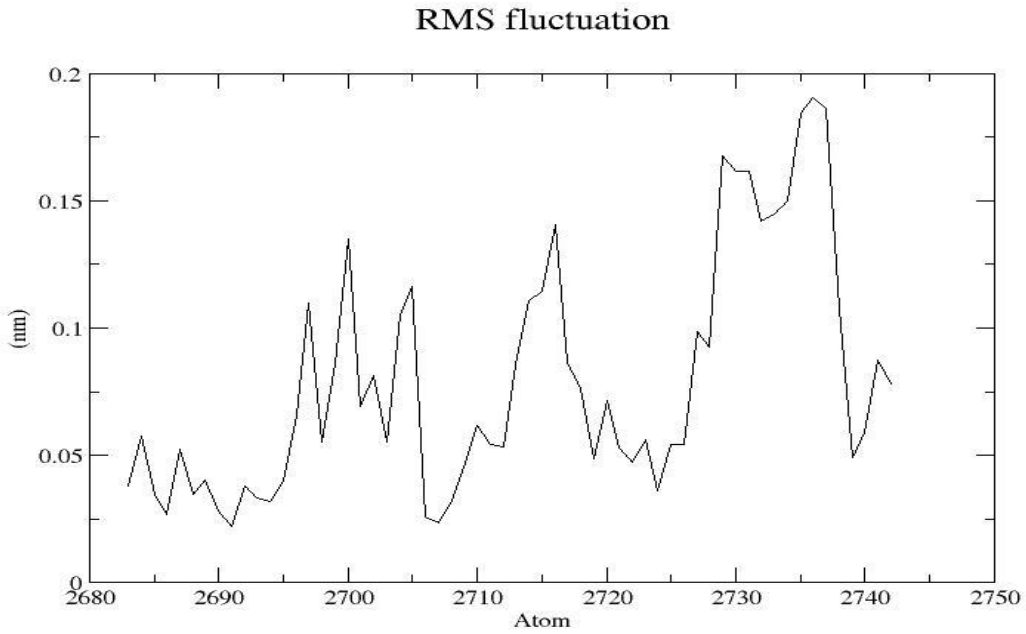

Fig 17: RMSF analysis in Olmesartan

The graph analyses the RMSF fluctuations of Olmesartan for 22ns.

The initial fluctuation was observed just below 0.05nm and then spike above 0.05nm and kept fluctuating till the end of time during the simulation.

The highest simulation was observed below 0.2nm on atom no. 2735. Hence it seems that the RMSF fluctuations of Olmesartan were not stable at the end of the time during simulation.

4.8.3 Radius of Gyration

A protein's radius of gyration in MD simulation is calculated to ascertain its compactness. The likelihood of a durable value for the radius of gyration is greatest if the protein structure is folded steadily (Rg). The value of the Radius of Gyration (Rg), on the other hand, progressively varies as a protein unfolds.

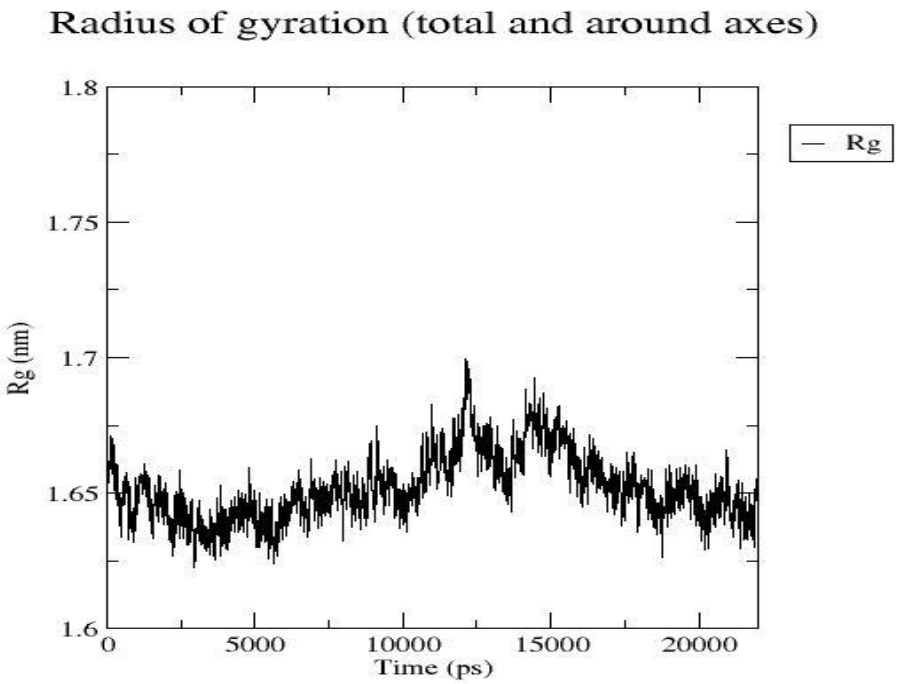

Fig 18: Radius of Gyration Analysis in Telmisartan

The graph analyses the radius of gyration of Telmisartan for 22ps.

The initial fluctuation was observed above 1.65nm and then went down. Again a spike in fluctuation was observed at 5000ps. The highest fluctuation was observed between 10,000 and 15,000 os which dropped just before 15,000ps. At the end of simulation the fluctuations were a bit stabe.

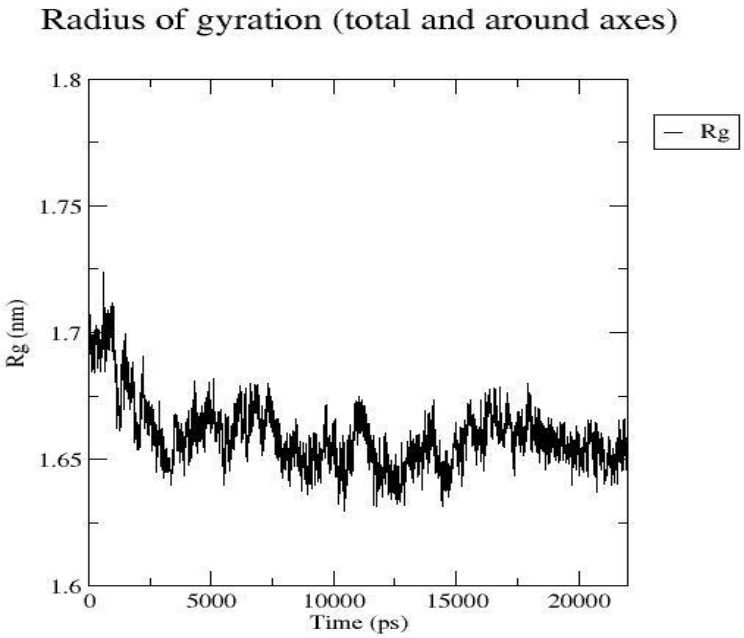

Fig 19: Radius of Gyration analysis in Olmesartan

The graph analyses the radius of gyration of Olmesartan for 22ps.

The initial fluctuations were observed just below 1.7nm and then dropped below 1.65nm at 2600ps. The fluctuations were observed till 15,000ps and got stable after that till the end of simulation i.e. 20,000ps.

4.8.4 Solvent Accessible Surface Area (SASA)

Proteins' Solvent Accessible Surface Area (SASA) is one factor that is used to analyse protein folding and stability. It is typically described as having a protein sphere surrounding the surface.

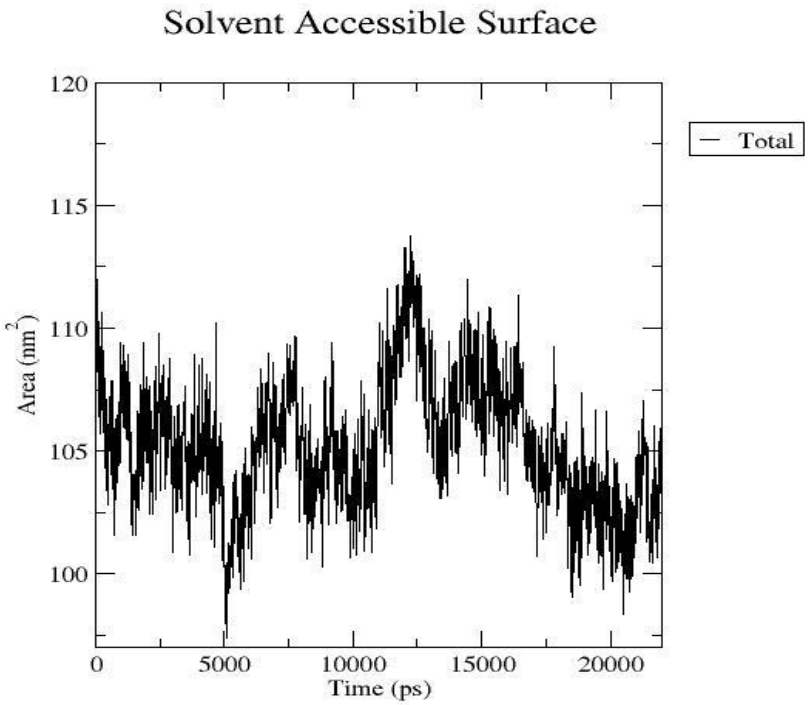

Fig 20: SASA analysis in Telmisartan

SASA was performed for the hydrophobic interactions of protein molecule.

The initial fluctuation was observed at 110nm and dropped at 0nm for 5000ps. The highest fluctuations observed below 115nm and then kept fluctuating. It dropped at 100nm for 20,000ps.

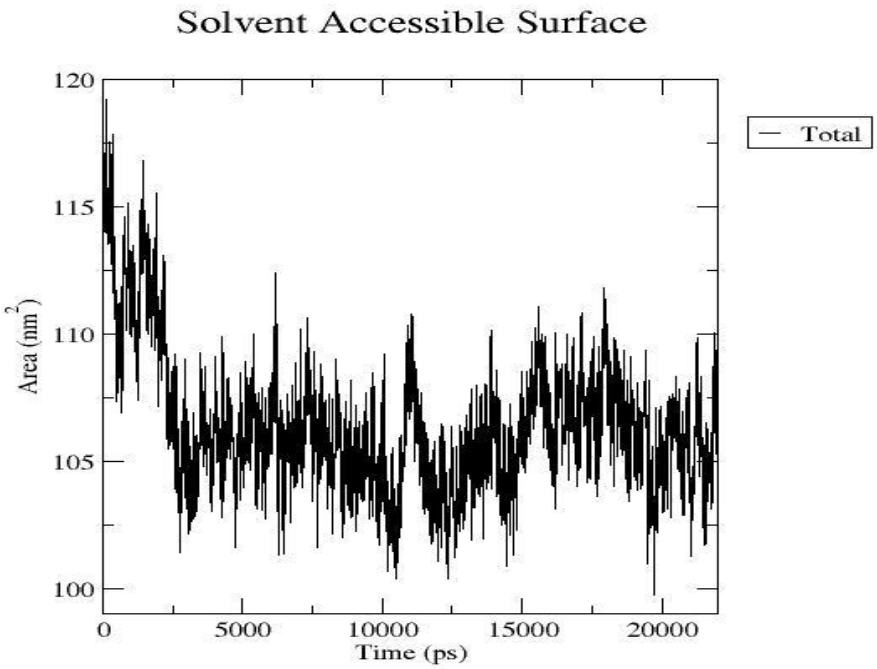

Fig 21: SASA analysis in Olmesartan

SASA was performed for the hydrophobic interactions of protein molecule. The initial fluctuation was observed between 115-120nm2 which was also the highest fluctuation observed during the simulation. The fluctuation dropped around 103nm2 between 2500-5000ps. Highest fluctuations were observed during the simulation and no stability was seen.

Angiotensin II receptor blocker Telmisartan (ARB) came out as the best docked and stable compound that can act as an Interleukin-6 inhibitor so as to cure COVID-19.

Our molecular docking and molecular dynamic simulation results have demonstrated that telmisartan has the best interactions with 1il6, as well as the best druggability qualities and energetically stable conformations. As shown in Fig 14 RMSD graph of Telmisartan, there were fluctuations in the graph but after 12ns it becomes stable whereas RMSD graph of olmesartan as depicted in Fig 15 is not stable. No stability was seen in sasa plot but it was better than Olmesartan as Telmisartan had lesser fluctuations in the beginning.

This study demonstrated the possibility of conventional drugs to treat SARS-CoV-2 infection by inhibiting interleukin-6. The chemicals that are produced have a strong potential for usage as therapeutic candidates. However, more thorough screening along with experimental findings may also confirm the findings of the current study and may create new opportunities for the development of drugs to treat SARS-CoV-2 infection in the future.

CHAPTER-6 CONCLUSION

In the present study, we executed compounds identification that can act as interleukin-6 inhibitors. Virtual Screening of 10 compounds was done by molecular docking, ADMET properties and drug likeness predictions of the natural compounds were performed using admetSAR and SwissADME. Docking resulted in the best docked complexes with lowest binding energies that were further subjected to molecular dynamics simulation using the GROMACS 2020.1 software analysis to confirm its stability. RMSD, RMSF, Radius of Gyration and SASA plots were investigated for analysis of stability of the docked complex so that we can identify the best compound for interleukin-6 inhibition. Main objective of this study was to do analysis of compounds that can act as il-6 inhibitors and can cure COVID-19. The study suggests that Telmisartan can act as Interleukin-6 inhibitor which can help in curing COVID-19 as Telmisartan was stable a complex when underwent simulation and had less fluctuations as compared to Olmesartan. As, COVID-19 became a life threatening disease, it was very crucial to analyse compounds and inhibit the interleukin-6.

CHAPTER-7 REFERENCES

1- Loeffelholz, M. J., & Tang, Y. W. (2020). Laboratory diagnosis of emerging human coronavirus infections–the state of the art. *Emerging microbes & infections*, *9*(1), 747-756.

2- Rodriguez-Morales, A. J., Cardona-Ospina, J. A., Gutiérrez-Ocampo, E., Villamizar-Peña, R., Holguin-Rivera, Y., Escalera-Antezana, J.P,... & Sah, R. (2020). Clinical, laboratory and imaging features of COVID-19: A systematic review and meta-analysis. *Travel medicine and infectious disease, 34,* 101623.

3- Wu, A., Peng, Y., Huang, B., Ding, X., Wang, X., Niu, P., ... & Jiang, T. (2020). Genome composition and divergence of the novel coronavirus (2019-nCoV) originating in China. *Cell host & microbe*, *27*(3), 325-328.

4- Huang, C., Wang, Y., Li, X., Ren, L., Zhao, J., Hu, Y., ... & Cao, B. (2020). Clinical features of patients infected with 2019 novel coronavirus in Wuhan, China. *The lancet*, *395*(10223), 497-506.

5- Channappanavar, R., Zhao, J., & Perlman, S. (2014). T cell-mediated immune response to respiratory coronaviruses. *Immunologic research*, *59*(1), 118-128.

6- Rabi, F. A., Al Zoubi, M. S., Kasasbeh, G. A., Salameh, D. M., & Al-Nasser, A. D. (2020). SARS-CoV-2 and coronavirus disease 2019: what we know so far. *Pathogens*, *9*(3), 231.

7- Akdis, M., Burgler, S., Crameri, R., Eiwegger, T., Fujita, H., Gomez, E., ... & Akdis, C. A. (2011). Interleukins, from 1 to 37, and interferon-γ: receptors, functions, and roles in diseases. *Journal of allergy and clinical immunology*, *127*(3), 701-721.

8- Zhu, Z., Wang, D., Jiao, W., Chen, G., Cao, Y., Zhang, Q., & Wang, J. (2017). Bioinformatics analyses of pathways and gene predictions in IL-1α and IL-1β knockout mice with spinal cord injury. *Acta Histochemica*, *119*(7), 663-670.

9- Belghith, M., Bahrini, K., Kchaou, M., Maghrebi, O., Belal, S., & Barbouche, M. R. (2018). Cerebrospinal fluid IL-10 as an early stage discriminative marker between multiple sclerosis and neuro-Behçet disease. *Cytokine*, *108*, 160-167.

10- Kishimoto, T. (2006). Interleukin-6: discovery of a pleiotropic cytokine. *Arthritis research & therapy*, *8*(2), 1-6.

11- Gabay, C. (2006). Interleukin-6 and chronic inflammation. *Arthritis research & therapy*, *8*(2), 1-6.

12- Nishimoto, N., & Kishimoto, T. (2006). Interleukin 6: from bench to bedside. *Nature clinical practice Rheumatology*, *2*(11), 619-626.

13- Heinrich, P. C., Behrmann, I., Haan, S., Hermanns, H. M., Müller-Newen, G., & Schaper, F. (2003). Principles of interleukin (IL)-6-type cytokine signalling and its regulation. *Biochemical journal*, *374*(1), 1-20.

14- Scheller, J., & Rose-John, S. (2006). Interleukin-6 and its receptor: from bench to bedside. *Medical microbiology and immunology*, *195*(4), 173-183.

15- Danwang, C., Endomba, F. T., Nkeck, J. R., Wouna, D. L. A., Robert, A., & Noubiap, J. J. (2020). A meta-analysis of potential biomarkers associated with severity of coronavirus disease 2019 (COVID-19). *Biomarker research*, *8*(1), 1-13.

16- Ponti, G., Maccaferri, M., Ruini, C., Tomasi, A., & Ozben, T. (2020). Biomarkers associated with COVID-19 disease progression. *Critical reviews in clinical laboratory sciences*, *57*(6), 389-399.

17- Herold, T., Jurinovic, V., Arnreich, C., Lipworth, B. J., Hellmuth, J. C., von Bergwelt-Baildon, M., ... & Weinberger, T. (2020). Elevated levels of IL-6 and CRP predict the need for mechanical ventilation in COVID-19. *Journal of Allergy and Clinical Immunology*, *146*(1), 128-136.

18- Magro, G. (2020). SARS-CoV-2 and COVID-19: Is interleukin-6 (IL-6) the 'culprit lesion'of ARDS onset? What is there besides Tocilizumab? SGP130Fc. *Cytokine: X*, *2*(2), 100029.

19- Kang, S., Tanaka, T., Narazaki, M., & Kishimoto, T. (2019). Targeting interleukin-6 signaling in clinic. *Immunity*, *50*(4), 1007-1023.

20- Aziz, M., Fatima, R., & Assaly, R. (2020). Elevated interleukin-6 and severe COVID-19: a meta-analysis. *Journal of medical virology*.

21- Johnson, D. E., O'Keefe, R. A., & Grandis, J. R. (2018). Targeting the IL-6/JAK/STAT3 signalling axis in cancer. *Nature reviews Clinical oncology*, *15*(4), 234-248.

22- Tanaka, T., Narazaki, M., & Kishimoto, T. (2016). Immunotherapeutic implications of IL-6 blockade for cytokine storm. *Immunotherapy*, *8*(8), 959-970.

23- Wu, Y., Xu, X., Chen, Z., Duan, J., Hashimoto, K., Yang, L., ... & Yang, C. (2020). Nervous system involvement after infection with COVID-19 and other coronaviruses. *Brain, behavior, and immunity*, *87*, 18-22.

24- Guaraldi, G., Meschiari, M., Cozzi-Lepri, A., Milic, J., Tonelli, R., Menozzi, M., ... & Mussini, C. (2020). Tocilizumab in patients with severe COVID-19: a retrospective cohort study. *The Lancet Rheumatology*, *2*(8),e474-e484.

25- Ulhaq, Z. S., & Soraya, G. V. (2020). Interleukin-6 as a potential biomarker of COVID-19 progression. *Medecine et maladies infectieuses*, *50*(4), 382.

26- Grifoni, A., Weiskopf, D., Ramirez, S. I., Mateus, J., Dan, J. M., Moderbacher, C. R., ... & Sette, A. (2020). Targets of T cell responses to SARS-CoV-2 coronavirus in humans with COVID-19 disease and unexposed individuals. Cell, 181(7), 1489-1501.

27- Atal, S., & Fatima, Z. (2020). IL-6 inhibitors in the treatment of serious COVID-19: a promising therapy?. *Pharmaceutical medicine*, *34*(4), 223-231.

28- Scheller, J., Chalaris, A., Schmidt-Arras, D., & Rose-John, S. (2011). The pro-and anti-inflammatory properties of the cytokine interleukin-6. *Biochimica et Biophysica Acta (BBA)-Molecular Cell Research*, *1813*(5), 878-888.

29- Chomarat, P., Banchereau, J., Davoust, J., & Karolina Palucka, A. (2000). IL-6 switches the differentiation of monocytes from dendritic cells to macrophages. *Nature immunology*, *1*(6), 510-514.

30- Mani, N. S., Budak, J. Z., Lan, K. F., Bryson-Cahn, C., Zelikoff, A., Barker, G. E., ... & Cohen, S. A. (2020). Prevalence of coronavirus disease 2019 infection and outcomes among symptomatic healthcare workers in Seattle, Washington. *Clinical Infectious Diseases*, *71*(10), 2702-2707.

31- Trott, O., & Olson, A. J. (2010). AutoDock Vina: improving the speed and accuracy of docking with a new scoring function, efficient optimization, and multithreading. *Journal of computational chemistry*, *31*(2), 455-461.

32- Huang, J., Rauscher, S., Nawrocki, G., Ran, T., Feig, M., De Groot, B. L., ... & MacKerell, A. D. (2017). CHARMM36m: an improved force field for folded and intrinsically disordered proteins. *Nature methods*, *14*(1), 71-73.

Ouriginal
by Turnitin

Document Information

Analyzed document	Eva Rathi Thesis Plag.docx (D142483837)
Submitted	7/28/2022 8:36:00 AM
Submitted by	Atul Kumar Upadhyay
Submitter email	atul.upadhyay@thapar.edu
Similarity	0%
Analysis address	atul.upadhyay.thapar@analysis.urkund.com